

AXISYMMETRIC VORTEX BREAKDOWN IN AN ENCLOSED CYLINDER FLOW.

by J. M. LOPEZ*

Aeronautical Research Laboratory,
P. O. Box 4331, Melbourne, Vic., 3001, Australia.

1. Introduction

The attraction of the confined swirling flow generated inside an enclosed cylinder by the constant rotation of one of its endwalls to a study of vortex breakdown is that the flow is defined by only four variables, these being the height H and radius R of the cylinder, the constant angular speed of rotation of the endwall Ω and the kinematic viscosity ν . These four variables are used to define two non-dimensional parameters which completely specify the flow conditions — the aspect ratio H/R and a rotational Reynolds number $Re = \Omega R^2/\nu$. The boundary conditions are also defined precisely since the flow is confined in a fixed volume. As Re and/or H/R are increased beyond critical values, the central vortex core undergoes breakdown.

Experimental investigations of this flow (eg. Vogel 1968, Escudier 1984, Roesner - private communication) have shown that it remains axisymmetric over a large range of the governing parameters, permitting the axisymmetric formulation of the Navier-Stokes equations to be solved using a time-accurate explicit finite-difference technique (Lopez 1987). Extensive comparisons with experiments at steady state have shown excellent agreement (Lopez 1987, 1988). There is also very good agreement with the numerical results of Lugt & Abboud (1987) who employed an implicit numerical technique.

So far, little work has been presented on the time scales of the flow evolution. Published experimental results have concentrated on the flow at steady state. Here, the time evolution is investigated numerically for the particular case of $H/R = 2.5$, which has a richness of flow phenomena as Re is varied. The flow is started from rest at $t = 0$ when the endwall is impulsively set to rotate at constant angular speed Ω . The evolution is studied with the aid of graphically animated sequences of the contours of the streamfunction ψ , azimuthal component of vorticity η and the angular momentum $\Gamma = rv$. The advection and diffusion of the angular momentum and azimuthal vorticity into the interior flow from the Ekman boundary layer on the rotating endwall is observed, as is the formation of the central vortex which eventually undergoes breakdown. Depending on the values of the governing parameters the transient oscillations are either damped, in which case the flow settles down to a steady state, or for higher Re , as the initial transients slowly decay, a new oscillation with a higher frequency is excited and the flow remains oscillatory. This oscillatory behavior is mostly confined to the central vortex region.

2. Governing Equations and Method of Solution

The assumption of axial symmetry is imposed on the flow in order to keep the numerics tractable. When the flow is steady, this assumption is satisfied, as is borne out by the experimental investigations (eg. Escudier, 1984). Small non-axisymmetric perturbations on these solutions will be damped. However, we are interested in the situation where the flow does not become steady. In this case there is the possibility of the flow becoming non-axisymmetric. There is very little experimental information on this regime of the flow and there are, to the author's knowledge, no three-dimensional computations of this flow. In the cases where the axisymmetric solutions remain oscillatory, we have no knowledge regarding their stability to non-axisymmetric perturbations. However, from Escudier's experimental investigations, for the case of $H/R = 2.5$, $Re = 2765$ which is a periodic oscillatory case, the flow shows little departure from axial symmetry. So that at least up to $Re = 2765$, for $H/R = 2.5$, the unsteady solutions are stable to small non-axisymmetric perturbations. To quote Escudier (1984): "For values of $\Omega R^2/\nu$ just above this curve (the curve separating the steady and unsteady regime in the $\Omega R^2/\nu - H/R$ parameter space) the oscillation is periodic and axial. As the Reynolds number is increased the motion becomes disturbed and ultimately turbulent. For $H/R > 3.1$, the first sign of non-steady motion is a precession of the

* Present address:— NASA Ames Research Center, Moffett Field, CA. 94035, U.S.A.

lower breakdown structure." Hence, for the case of $H/R = 2.5$, there exists a range of Re for which the flow is oscillatory and axisymmetric. Unfortunately, there is no estimate of the Reynolds number at which the flow loses stability to non-axisymmetric perturbations. Fortunately, we can proceed to investigate the transition to unsteadiness for the case of $H/R = 2.5$ using the assumption of axial symmetry, knowing that at least for $Re \leq 2765$, the axisymmetric oscillatory solutions are stable.

The governing equations used are the unsteady axisymmetric Navier-Stokes equations, written in conservative streamfunction-vorticity form, with time and length scaled by Ω and $1/R$ respectively. The method of solution and details of the boundary conditions are given in Lopez (1988), where the accuracy of the method is also discussed.

3. Results and Discussion

When the cylinder aspect ratio is 2.5, for $Re < 1000$, the steady flow consists of an Ekman boundary layer on the rotating endwall pumping fluid radially outward in a spiral path. At the same time, fluid is drawn into the boundary layer from the interior to satisfy continuity. This centrifugal pumping, together with the presence of the cylinder sidewall, establishes a secondary overturning meridional flow which advects fluid from the Ekman layer, where it has acquired angular momentum and total head, into the interior of the flow. The fluid loses a proportion of its acquired angular momentum and total head through the action of viscous stresses in the boundary layers on the cylinder sidewall and on the stationary endwall. The boundary layer on the stationary endwall separates on the axis and forms a central vortex which returns the fluid to the Ekman boundary layer. The structure of this central vortex is primarily determined by the structure of the stationary endwall boundary layer, which for $Re < 1000$ is broad and diffuse. At these low Reynolds numbers, the central vortex is essentially cylindrical and its associated vorticity vector is primarily directed in the axial direction, with some azimuthal component due to the secondary overturning motion.

When Re is increased to 1600, a new feature is present in the steady flow field. The streamlines on the central vortex now show the features of a weak standing centrifugal wave, as can be seen in figure 1. The features and mechanics responsible for this behavior have been discussed at length in Lopez (1988) and Brown & Lopez (1988). In summary, at the higher Reynolds numbers, the structure of the stationary endwall boundary layer has changed such that its depth is reduced and its flow has larger gradients of angular momentum Γ , and total head H . The distribution of Γ and H in the central vortex, as it emerges from the stationary endwall boundary layer, is such that a region of azimuthal vorticity is generated by the tilt and stretch mechanism described in Brown & Lopez (1988), which induces a reversed axial velocity and an undulation in the central streamtubes. As Re is increased, this effect is enhanced and the induced reversed axial velocity is large enough to stagnate the axial flow. At $Re = 1918$, a small spherical recirculation bubble is evident on the axis. Figure 1 illustrates the changes in flow structure at steady state with Re . The direction of the meridional flow in figure 1 is downward. Of particular interest is the trend that the wavelength of the undulations is decreasing with increasing Re whilst their amplitudes increase and the stagnation point on the axis occurs further upstream. Also, the time taken to reach steady state increases with Re . Figure 2 illustrates the time history of the streamfunction at a particular point in the flow ($r = R/6$, $z = 2H/3$). For $Re = 2200$, the flow settles down to a steady state after approximately 700 rotations of the bottom endwall, whereas for $Re = 2400$ it took about 1200 rotations and about 2000 rotations for $Re = 2500$. For $Re = 2600$, the system was integrated out to 3000 rotations and there was still evidence of oscillations, however these were slowly damped. Up to this value of Re , Escudier (1984) reports that the experimental flow also settles down to a steady state and, provided $\Omega R^2/\nu$ is well below the value at which the flow becomes oscillatory (which for $H/R = 2.5$ is approximately 2600), the flow reached steady state when started from rest in ten's of seconds. In Escudier's experiment, Ω was typically of the order of ten revolutions per second. As the Reynolds number for unsteadiness was approached, Escudier reports that the time taken to reach steady state became very long. This is precisely the behavior indicated in figure 2.

From figures 1 and 2, we note that persistent oscillations, both damped and undamped, are associated with a bifurcation in the flow streamlines. For $Re < 2400$, the flow field at steady state consists of two individual recirculation bubbles located on the axis of symmetry. The vortical flow

between the two bubbles is similar in nature to that upstream of the leading bubble, however it has a larger vortex core and is less intense. This reconverged vortical flow poses a distribution of Γ and H which is responsible for the presence of the second bubble via the mechanism described earlier. However, when Re is increased beyond 2400, the two bubbles coalesce and the vortical flow past the leading bubble does not have a chance to reconverge fully. For $2400 < Re < 2600$, the coalescing of the two bubbles is not very great. There is still a considerable amount of reconvergence past the first bubble and the flow is able to find a steady equilibrium configuration after some time. For higher Re (eg. $Re = 2765$), no such steady equilibrium is found. In this case, the boundary layer flow on the endwalls and sidewall reaches steady state relatively quickly and the emergent central vortex undergoes breakdown further upstream than it does at lower Re , following the trend shown in figure 1. The resultant recirculation bubble is larger, as is the second bubble which forms in closer proximity to the leading bubble. This larger second bubble causes the vortical flow to diverge at a much larger r than it would have in the absence of the second bubble. The result is a very broad, near stagnant central vortex flow past the leading bubble. The subsequent distribution of Γ and H is not conducive to breakdown and hence the second recirculation bubble cannot be maintained and is seen to be washed downstream. As it is washed downstream, the vortical flow past the leading bubble is able to re-converge in the absence of the second bubble. The leading bubble is now closed at the downstream end by a stagnation point on the axis and the central vortex has a similar structure to that upstream of the leading bubble. The flow topology resembles that of lower Re cases where two individual bubbles are present. However, the reconverged central vortex is prone to a more pronounced breakdown and it does so in a manner which results in a re-coalescence of the two bubbles and the whole process repeats itself. The frequency of this oscillatory behavior is found from the power spectra in figure 3 and is f_1 . The oscillation, due to the interaction between the two bubbles, occurs approximately 27 times every 1000 rotations of the bottom endwall. It appears that the non-dimensional frequency f_1 , is independent of Re for the range considered (i.e. $2600 \leq Re \leq 4000$).

From the power spectra shown on the left hand side of figure 3, the transient oscillations due to the impulsive start have a frequency f_0 which is also independent of Re . Only the rate at which it is damped is Re dependent. At $Re = 4000$, there is still a weak signal due to f_0 in the spectra taken for $2000 \leq t \leq 3000$. For $Re < 3500$, the f_1 oscillation is the predominant mechanism responsible for the unsteadiness. However, at $Re = 3000$, there is a faint signal f_2 evident at late times and at $Re = 3500$ this f_2 signal is present at early times as well. At late times for $Re = 3500$, the power spectra clearly shows the non-linear interaction between the two incommensurate frequencies f_1 and f_2 and the corresponding time-series from figure 2 shows this situation as an almost chaotic signal. At $Re = 4000$, this new f_2 frequency dominates the time dependence of the flow solution, although there are still faint signals at f_0 and f_1 which have not completely died out at those times.

An examination of the streamfunction at various times allows an identification of the mechanism responsible for this new f_2 frequency which emerges at higher Re . At these higher Re , the central vortex undergoes vortex breakdown even closer to the stationary endwall, following the trend illustrated in figure 1. Also, the recirculation bubble is larger, as are the recirculating velocities inside the bubble. The effect of having this active recirculating bubble in such close proximity to the endwall is to increase the thickness of the endwall boundary layer. A particle of fluid which would have spiraled inward to a very small r in the absence of the bubble, now is diverted at a larger r and the result is a broader and less intense central vortex than would have been expected at the high Re values. Now, with a weakened central vortex, the active recirculation bubble cannot be maintained and it is washed downstream. In the absence of the bubble, the endwall boundary layer 'heals' and once again separates at $r = 0$ to form a tight intense central vortex which undergoes a violent breakdown and results in a large recirculation bubble. The whole process repeats itself with a frequency f_2 .

References

- Brown, G. L. & Lopez, J. M. 1988 *A.R.L. Aero. Report 174, AR-004-573, also submitted to J. Fluid Mech.*
- Escudier, M. P. 1984 *Experiments in Fluids* 2, 189-196.
- Lopez, J. M. 1987 *in press: Proc. Int. Sym. Comp. Fluid Dynamics (North Holland).*
- Lopez, J. M. 1988 *A.R.L. Aero. Report 173, AR-004-572, also submitted to J. Fluid Mech.*
- Lugt, H. J. & Abboud, M. 1987 *J. Fluid Mech.* 170, 179-200.
- Vogel, H. U. 1968 *Maz-Planck-Inst. Bericht* 6.

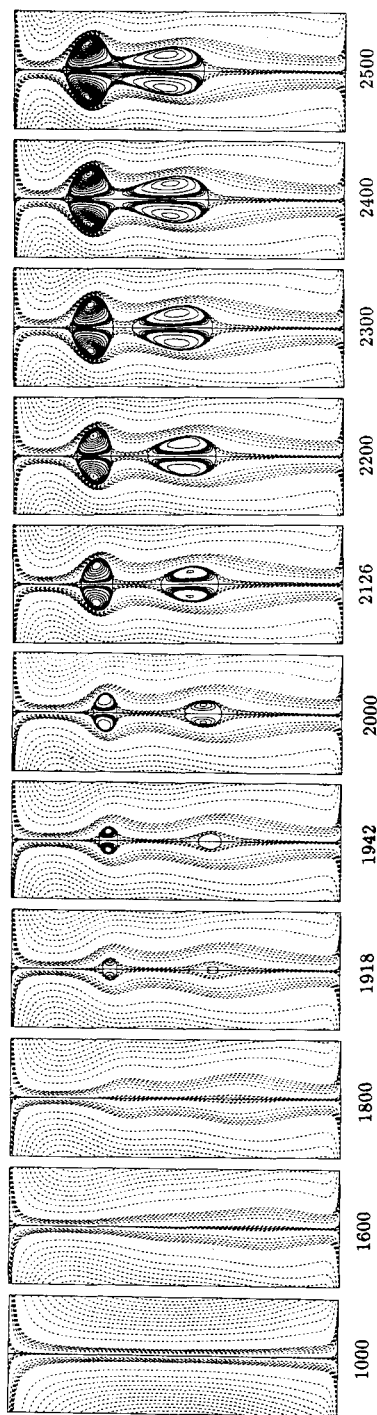


Fig. 1: Details of the streamfunction at steady state ($0 \leq r \leq 5R/12$) for $H/R = 2.5$ and Re as indicated.

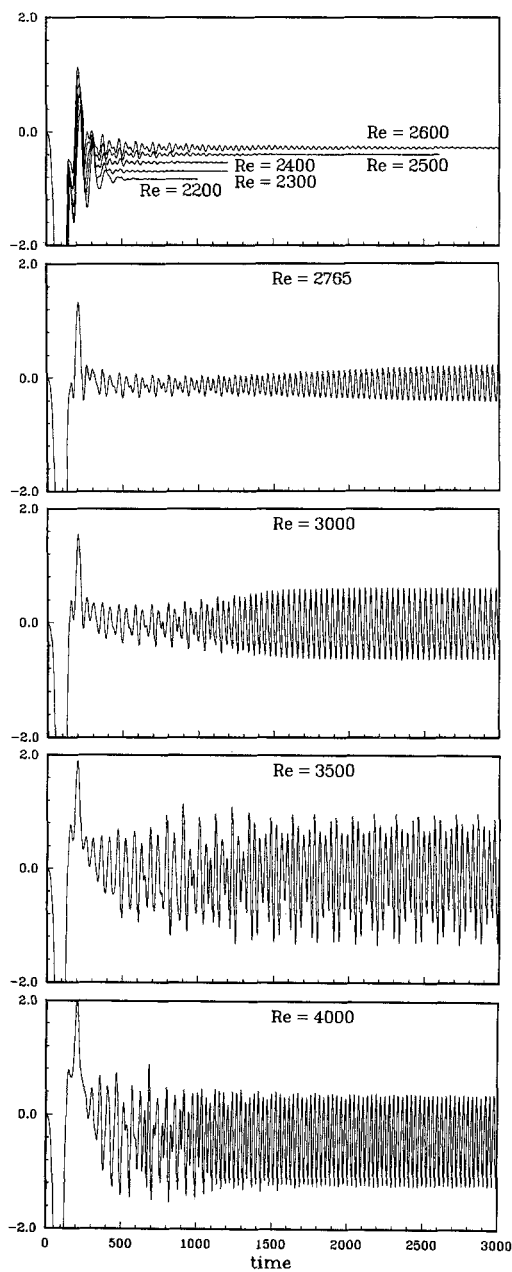


Fig. 2: Time history of the streamfunction at the point $r = R/6$, $z = 2H/3$ for $H/R = 2.5$ and Re as indicated. Time is scaled with Ω .

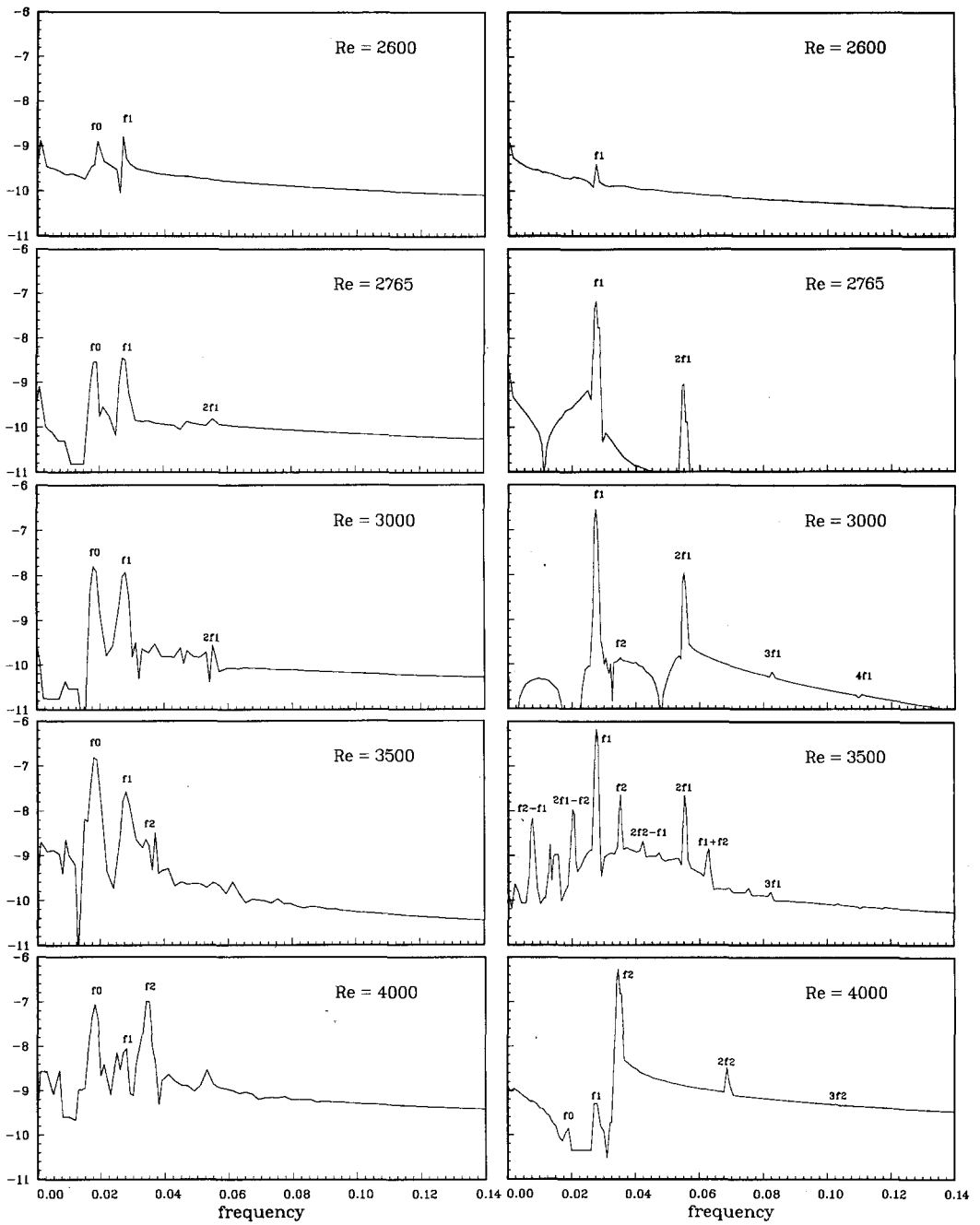


Fig. 3: \log_{10} of the power spectrum corresponding to the streamfunction time-series in Fig. 2. The spectra on the left hand side are for $500 \leq t \leq 1000$ and the spectra on the right hand side are for $2000 \leq t \leq 3000$. The frequency is scaled with $1/\Omega$.